European Journal of Pharmaceutics and Biopharmaceutics 141 (2019) 111–120

Contents lists available at ScienceDirect

European Journal of Pharmaceutics and Biopharmaceutics

journal homepage: www.elsevier.com/locate/ejpb

Research paper

Micro-scale solubility assessments and prediction models for active pharmaceutical ingredients in polymeric matrices

Esther S. Bochmann[a,c], Dirk Neumann[b], Andreas Gryczke[c], Karl G. Wagner[a,*]

[a] Department of Pharmaceutical Technology and Biopharmaceutics, University of Bonn, Bonn, Germany
[b] Scientific Consilience GmbH, Saarbrücken, Germany
[c] AbbVie Deutschland GmbH & Co. KG, Ludwigshafen, Germany

ARTICLE INFO

Chemical compounds studied in this article:
Bisacodyl (PubChem CID: 2391)
Carbamazepine (PubChem CID: 2554)
Celecoxib (PubChem CID: 2662)
Cilostazol (PubChem CID: 2754)
Clozapine (PubChem CID: 2818)
Dipyridamole (PubChem CID: 3108)
Felodipine (PubChem CID: 3333)
Gliclazide (PubChem CID: 3475)
Griseofulvin (PubChem CID: 441140)
Indomethacin (PubChem CID: 3715)
Itraconazole (PubChem CID: 55283)
Lamotrigine (PubChem CID: 3878)
Loratadine (PubChem CID: 3957)
Nifedipine (PubChem CID: 4485)
Naproxen (PubChem CID: 156391)
Posaconazole (PubChem CID: 468595)
Praziquantel (PubChem CID: 4891)
Probucol (PubChem CID: 4912)
Ritonavir (PubChem CID: 392622)
Telmisartan (PubChem CID: 65999)
Verapamil-HCl (PubChem CID: 62969)
Copovidone (PubChem CID: 25086-89-9)

Keywords:
Solubility
Data review
Amorphous solid dispersion
Prediction model

ABSTRACT

The number of models for assessing the solubility of active pharmaceutical ingredients (APIs) in polymeric matrices on the one hand and the extent of available associated data on the other hand has been rising steadily in the past few years. However, according to our knowledge an overview on the methods used for prediction and the respective experimental data is missing. Therefore, we compiled experimental data, the techniques used for their determination and the models used for estimating the solubility. Our focus was on polymers commonly used in spray drying and hot-melt extrusion to form amorphous solid dispersions (ASDs), namely polyvinylpyrrolidone grades (PVP), polyvinyl acetate (PVAc), vinylpyrrolidone-vinyl acetate copolymer (copovidone, COP), polyvinyl caprolactam-polyvinyl acetate-polyethylene glycol graft polymer (Soluplus®, SOL), different types of methacrylate copolymers (PMMA), polyethylene glycol grades (PEG) and hydroxypropylmethylcellulose grades (HPMC). The literature data were further supplemented by our own results. The final data set included 37 APIs and two sugar derivatives. The majority of the prediction models was constituted by the melting point depression method, dissolution endpoint measurements, indirect solubility determination by T_g and the use of low molecular weight analogues. We observed that the API solubility depended more on the working group which conducted the experiments than on the measuring technique used. Furthermore, this compilation should assist researchers in choosing a prediction method suited for their investigations.

Furthermore, a statistical assessment using recursive feature elimination was performed to identify descriptors of molecules, which are connected to the API solubility in polymeric matrices. It is capable of predicting the criterium 20% API soluble at 100 °C (Yes/No) for an unknown compound with a balanced accuracy of 71%. The identified 8 descriptors to be connected to API solubility in polymeric matrices were the number of hydrogen bonding donors, three descriptors related to the hydrophobicity of the molecule, glass transition temperature, fractional negative polar van der Waals surface area, out-of-plane potential energy and the fraction of rotatable bonds. Finally, in addition to our own model, the data set should help researchers in training their own solubility prediction models.

1. Introduction

In recent years, the increasing number of poorly soluble active pharmaceutical ingredients (APIs) led to the requirement of new and innovative strategies and dosage forms in drug formulation development [1]. One of the so-called enabling technologies to overcome poor API-solubility is the formation of amorphous solid dispersions (ASDs), either by solvent evaporation or by melting techniques (e.g. spray drying or hot-melt extrusion) [2-4]. In ASDs, the API is amorphously embedded (molecularly dispersed) in a polymeric matrix and often kinetically stabilized, especially if a supersaturated state at room temperature is achieved. Due to the absence of a crystal lattice, the API rate and extent of dissolution in aqueous media are increased and thus, the respective bioavailability is enhanced [5-8]. The drawback of a metastable amorphous API form, which is mainly kinetically stabilized in a polymeric matrix, is the overall reduced stability due to potential

* Corresponding author.
E-mail address: karl.wagner@uni-bonn.de (K.G. Wagner).

https://doi.org/10.1016/j.ejpb.2019.05.012
Received 18 December 2018; Received in revised form 28 March 2019; Accepted 13 May 2019
Available online 14 May 2019

recrystallisation over the shelf life and the ensuing decrease in bioavailability [5,9]. Therefore, a thermodynamically embedded amorphous API in a polymeric matrix, which is entirely soluble without supersaturation at room temperature, is favourable. This can be achieved if the API content in an (dissolved) ASD is completely soluble in the investigated polymeric matrix at ambient conditions [10,11]. It leads not only to a kinetically but more to a thermodynamically stabilized system which prevents recrystallization and thus prolongs the shelf life of the entire drug formulation [3,12-14]. However, the measurement of the API solubility is challenging and a direct determination at room temperature is obstructed by the high viscosity of the overall system [12]. The slow kinetics of such systems result in unrealistically long periods to observe recrystallization and determine the limit of API solubility, respectively. Therefore, either the use of surrogate systems with a low weight analogue to the respective polymer or measurements at elevated temperatures and subsequent extrapolation to room temperature are used to obtain the desired information on an experimental basis [9,15-17].

Several techniques and assumptions, with corresponding data sets, are available in the literature which can be used to elucidate the solubility of an API in a given polymeric matrix [5,10,12,15]. Since the API solubility cannot be directly measured at room temperature, these models predict the solubility with different strategies. Commonly used techniques are based on differential scanning calorimetry (DSC) methods or measurements in low molecular weight analogues. The most widely investigated DSC methods include DSC measurements, the melting point depression method [10,17,18] and the dissolution endpoint method [19-21]. During measurement and while applying a sufficiently low heating rate to the specimen, either the onset or the endset of the melting endotherm can be analysed. Furthermore, indirect measurements of the API solubility in polymeric matrices by using the glass transition temperature (T_g) of recrystallized or annealed samples have been reported [22,23]. Further measuring techniques, which make use of heat capacity differences between the solid solution and its unmixed components, solution calorimetry or high-energy mechanical milling on processed solid dispersions have also been investigated [24-26]. In the case of measurements in low molecular weight analogous, the limiting factor of the high viscosity of an ASD at room temperature is circumvented by employing the polymer's low molecular weight analogue and extrapolating the obtained solubility to the polymer of interest [27,28].

However, most of the data sets used to train solubility prediction methods encompass only one or a limited number of APIs. The predictive accuracy of such models might hence, be limited. The aim of our study is (1) to compare the available data sets and models published so far and (2) to supplement these data with our own work and data on assessing API solubility in polymeric matrices. This leads to a compilation of API-polymer solubility data, which should assist researchers in choosing an adequate prediction method and should provide researchers with a data set for training solubility prediction models. Finally, we were able to prove the validity of our own DSC method by comparing it to a wide data set, based on other methods presented in literature.

2. Material and methods

2.1. Material

Bisacodyl, dipyridamole, gliclazide, naproxen and verapamil-HCl were received from Sigma-Aldrich Chemical Co. (St. Louis, MO, USA). Griseofulvin, indomethacin and itraconazole were obtained from Alfa Aesar GmbH & Co. KG (Karlsruhe, Germany). Clozapine, ritonavir and posaconazole were received from Swapnroop Drug and Pharmaceuticals (Aurangabad, India). Loratadine and telmisartan were purchased from sris Pharmaceuticals (Telangana, India). Nifedipine and probucol were from Cayman Chemical (Ann Arbor, MI, USA). Celecoxib was purchased from Cadila Pharmaceuticals Ltd. (Ahmedabad, India) and cilostazol was received from Amsal Chem Pvt Ltd. (Mumbai, India). Felodipine was obtained from Molekula Limited (Newcastle, UK), lamotrigine was received from Maps Laboratories Pvt. Ltd. (Gujarat, India), praziquantel was received from Divis Laboratories Ltd. (Telangana India). Vinylpyrrolidone-vinyl acetate copolymer (copovidone, Kollidon® VA 64, COP), polyvinyl caprolactam-polyvinyl acetate-polyethylene glycol graft polymer (Soluplus®, SOL) and carbamazepine were kindly donated by BASF SE (Ludwigshafen, Germany) (Table 1).

Table 1
Physicochemical properties of substances under investigation. Molecular weight was taken from PubChem Substance and Compound databases [29], all other parameters were experimentally determined.

Substance	*MW* [g/mol]	T_m [°C]	T_g [°C]	C_p step at T_g [J/g·K]	Soluble in COP at 100 °C
Bisacodyl	361.4	133.6	16.1	0.36	Yes
Carbamazepine	236.3	175.1 190.2	52.7	0.38	No
Celecoxib	381.4	160.9	56.8	0.39	Yes
Cilostazol	369.5	158.6	31.2	0.46	No
Clozapine	326.8	182.1	59.7	0.35	No
Dipyridamole	504.6	167.1	38.2	0.68	Yes
Felodipine	384.3	144.2	45.0	0.30	Yes
Gliclazide	323.4	170.5	39.6	0.48	No
Griseofulvin	352.8	218.3	88.9	0.30	No
Indomethacin	357.8	160.1	44.4	0.33	Yes
Itraconazole	705.6	165.8	57.7	0.44	No
Lamotrigine	256.1	215.8	93.3	0.54	No
Loratadine	382.9	134.6	34.9	0.30	No
Naproxen	230.3	156.1	6.7*	0.31*	Yes
Nifedipine	346.3	172.2	44.3	0.34	Yes
Posaconazole	700.8	167.7	59.8	0.43	No
Praziquantel	312.4	138.3	35.9	0.37	No
Probucol	516.8	126.3	25.6	0.46	Yes
Ritonavir	720.9	121.8	48.6	0.46	Yes
Telmisartan	514.6	268.3	129.5	0.35	No
Verapamil-HCl	491.1	142.3	55.2	0.51	No
Copovidone (COP)	45,000–70,000	–	107	0.40	–
Soluplus® (SOL)	90,000–140,000	–	71.1	0.30	–

* measured with 10% COP weight fraction due to APIs recrystallization tendency.

2.2. Methods

2.2.1. Differential scanning calorimetry (DSC)

A DSC 2 from Mettler Toledo (Gießen, Germany) was used to analyse glass transition temperatures (T_gs), heat capacity steps at T_g and the API solubility in polymer melts. The system was equipped with an auto sampler, nitrogen cooling and nitrogen as purge gas (30 ml/min). Calibration of the DSC was performed by using n-octane, indium and zinc standards. Every investigated material was analysed in triplicate placing approx. 10 mg sample in a 40 µl aluminium pan with a pierced lid and using 10 K/min as heating and cooling rate. In the case of heat capacities, measurements were conducted against a sapphire standard and in TOPEM® mode (modulated DSC) with 1 K pulse height, 15–30 s pulse width and an underlying heating rate of 2 K/min. For heat capacity measurement, the samples were annealed prior to analysis to enable homogeneous API-distribution in the polymeric matrix. Before conducting any DSC measurement, samples were prepared by using a MM400 ball mill of Retsch GmbH (Haan, Germany) with 30 Hz and 3x 5 min milling cycles.

2.2.2. Solubility determination via DSC

As the solubility determination of APIs in COP and SOL were conducted by using a protocol from our recent work; the description of the method can be found in complete detail there [23].The method was based on an indirect measurement of the API solubility by using the T_g.

Table 2
Solubility Review in (w/w) at 25 °C (Methods: Index 1 = Melting point depression method; Index 2 = Dissolution endpoint method; Index 3 = Indirect solubility determination by T_g; Index 4 = Measurement in low molecular weight analogues; Index 5 = others; Polmers: PVP (K-value); COP (PVP:PVAc ratio); PEG (molecular weight); PMMA (EPO: Eudragit® E PO/E100: Eudragit® E100/L100: Eudragit® L100); HPMC (E5: Ethocel® E5/AS: HPMC acetate succinate)).

API	Polymer						
	PVP	PVAc	COP	SOL	PEG	PMMA	HPMC
Aceclofenac				0.27[1] [58]			
Acetaminophen	0.17[5] (K17) [54]	0.00[4] [53]	0.21[2] (6:4) [21,47]	0.04[1] [54]			0.02[2] (AS) [55]
	0.18[4] (K17) [53]	0.01[1] [54]	0.28[2] (6:4) [47,55]	0.09[5] [54]			
	0.19[5] (K17) [54]	0.01[5] [54]	0.02[2] (3:7) [53]	0.10[5] [54]			
	0.23[2] (K25) [21,47]	0.01[5] [54]	0.03[3] (3:7) [53]				
	0.29[1] (K17) [54]		0.05[1] (3:7) [53]				
	0.32[2] (K25) [47,55]		0.05[4] (3:7) [53]				
Albendazole			0.04[1] (6:4) [59]	0.06[1] [59]		0.02[1] (EPO) [59]	
Bisacodyl			0.08[3] (6:4)	0.22[3]			
Carbamazepine	0.02[3] (K12) [51]		0.00[3] (6:4)	0.00[1] [42]			
				0.00[3]			
Celecoxib	0.38[3] (K12) [51]	0.02[3] [50]	0.06[2] (6:4) [53]	0.09[3]		0.20[5] (EPO) [26]	0.25[3] [51]
	0.38[5] (K17) [54]	0.03[4] [50,53]	0.17[3] (6:4) [53]	0.23[5] [54]		0.41[1] (EPO) [26]	0.32[1] [51]
	0.38[5] (K17) [54]	0.08[1] [54]	0.25[1] (6:4) [53]	0.23[5] [54]			
	0.40[3] (K12) [50]	0.13[5] [54]	0.26[4] (6:4) [53]	0.25[1] [54]			
	0.41[4] (K17) [53]	0.16[5] [54]	0.33[3] (6:4)	0.29[1] [51]			
	0.43[1] (K17) [54]		0.33[3] (6:4) [50]	0.34[3] [51]			
	0.44[1] (K12) [51]		0.38[4] (6:4) [50]				
	0.60[4] (K12) [50]						
			0.08[3] (3:7) [50]				
			0.18[4] (3:7) [50]				
			0.20[3] (5:5) [50]				
			0.26[4] (5:5) [50]				
			0.36[3] (7:3) [50]				
			0.42[4] (7:3) [50]				
Chloramphenicol	0.39[5] (K17) [54]	0.00[4] [53]	0.05[2] (5:5) [53]	0.11[5] [54]			
	0.40[5] (K17) [54]	0.04[1] [54]	0.14[3] (5:5) [53]	0.14[1] [54]			
	0.40[1] (K17) [54]	0.05[5] [54]	0.15[1] (5:5) [53]	0.14[5] [54]			
	0.52[4] (K17) [53]	0.06[5] [54]	0.26[4] (5:5) [53]				
Cilostazol	0.00[1] (K29/32) [60]		0.00[1] (6:4) [60]	0.00[3]			0.00[1] (E5) [60]
			0.00[3] (6:4)				
Cinnarizine	0.01[1] (K30) [61]			0.00[1] [16]			
Clozapine			0.00[3] (6:4)	0.00[3]			
Curcumin	0.00[1] (K90) [62]				0.00[1] (8000) [62]	0.00[1] (EPO) [62]	0.00[1] (E5) [62]
Dipyridamole	0.00[1] (K30) [61]		0.03[3] (6:4) [23]	0.18[3] [23]			
Felodipine	0.00[2] (K25) [43]	0.00[2] [52]	0.00[2] (6:4) [43]	0.00[2] [63]		0.00[2] (EPO) [64]	0.00[2] (AS) [63]
	0.03[2] (K15) [43]	0.04[4] [53]	0.11[2] (6:4) [52]	0.20[3]		0.20[5] (EPO) [26]	
	0.05[4] (K17) [53]		0.22[3] (6:4)			0.31[1] (EPO) [26]	
	0.06[1] (K17) [53]		0.30[5] (6:4) [26]				
	0.07[2] (K12) [43]		0.42[1] (6:4) [26]				
	0.07[4] (K12) [27]						
	0.07[3] (K17) [53]						
	0.07[4] (K29/32) [27]						
	0.07[4] (K90) [27]						
	0.08[2] (K17) [53]						
	0.10[2] (K15) [63]						
	0.18[5] (K29/32) [25]						
	0.24[2] (K25) [52]						
	0.25[4] (K29/32) [39]						
	0.31[4] (K12) [39]						
Gliclazide			0.00[3] (6:4)	0.08[3]			
Griseofulvin	0.09[5] (K30) [24]		0.00[3] (6:4)	0.00[3]		0.09[5] (E100) [24]	
						0.12[5] (L100) [24]	
Ibuprofen	0.50[2] (K25) [52]	0.05[2] [52]	0.41[2] (6:4) [52]				
Ibuprofen sodium			0.00[2] (6:4) [21]	0.00[2] [21]			

(*continued on next page*)

Table 2 (*continued*)

API	Polymer						
	PVP	PVAc	COP	SOL	PEG	PMMA	HPMC
Indomethacin	0.08[5] (K30) [24] 0.13[4] (K90) [27] 0.13[4] (K29/32) [27] 0.14[4] (K12) [27] 0.20[1] (K30) [65] 0.27[1] (K12) [65] 0.30[3] (K12) [22] 0.31[4] (K17) [53] 0.31[4] (K25) [66] 0.31[4] (K30) [66] 0.31[4] (K90) [66] 0.33[4] (K12) [66] 0.39[3] (K30) [66] 0.40[3] (K12) [66] 0.40[3] (K90) [66] 0.41[3] (K25) [66] 0.41[5] (K29/32) [25] 0.43[2] (K12, K15) [19-21] 0.43[2] (K25) [46] 0.54[1] (K12) [51] 0.54[3] (K12) [51]	0.00[1] [65] 0.00[2] [19-21] 0.01[2] [46] 0.01[4] [53]	0.31[1] (6:4) [65] 0.32[2] (6:4) [19-21] 0.33[1] (6:4) [18] 0.34[2] (6:4) [46] 0.36[3] (6:4) [23] 0.06[2] (7:3) [53] 0.19[3] (7:3) [53] 0.22[4] (7:3) [53] 0.35[1] (7:3) [53] 0.21[2] (3:7) [46]	0.20[3] [51] 0.26[3] [23] 0.31[1] [51]	0.22[2] (6000) [44] 0.25[2] (35000) [44]	0.09[5] (E100) [24] 0.10[5] (L100) [24]	0.08[3] [51] 0.27[1] [51]
Itraconazole	0.09[5] (K30) [24]		0.00[2] (6:4) [21] 0.00[3] (6:4) [23]	0.00[2] [21] 0.00[3] [23]	0.00[1] (6000) [67]	0.08[5] (E100) [24] 0.13[5] (L100) [24]	
Ketoconazole	0.01[4] (K12) [27] 0.01[4] (K29/32) [27] 0.01[4] (K90) [27]						0.00[2] [68]
Lacidipine	0.00[1] (K12) [65] 0.00[1] (K30) [65]	0.00[1] [65]	0.00[1] (6:4) [65]		0.05[1] (8000) [65] 0.22[1] (10000) [65]		
Loratadine			0.00[3] (6:4)	0.00[3]			
Mannitol	0.00[2] (K12, K15) [19-21]						
Naproxen	0.06[4] (K12) [17] 0.06[4] (K25) [17] 0.06[4] (K90) [17] 0.31[2] (K25) [21,47] 0.31[2] (K25) [47,55] 0.36[2] (K25) [46]	0.01[2] [46]	0.19[2] (6:4) [46] 0.21[2] (6:4) [47,55] 0.25[3] (6:4) 0.28[2] (6:4) [21,47] 0.07[2] (3:7) [46]	0.32[3]			0.03[2] (AS) [55]
Nifedipine	0.05[4] (K12) [27] 0.05[4] (K29/32) [27] 0.05[4] (K90) [27] 0.06[4] (K29/32) [39] 0.07[4] (K12) [39] 0.21[2] (K12) [19-21]	0.00[2] [20,21]	0.12[2] (6:4) [19-21] 0.19[3] (6:4) [23]	0.05[1] [69] 0.23[3] [23]			
Posaconazole			0.00[3] (6:4)	0.00[3]			
Praziquantel			0.00[3] (6:4)	0.00[3]			
Probucol			0.14[3] (6:4)	0.13[3]			
Ritonavir	0.26[1] (K12) [51]		0.03[3] (6:4)	0.00[3] 0.00[1] [51]			
Sucrose	0.02[4] (K12) [27] 0.02[4] (K29/32) [27] 0.02[4] (K90) [27]				0.00[1] (6000) [41]		
Sulfadiazine	0.00[2] (K17) [70]			0.00[2] [70]			
Sulfadimidine	0.18[2] (K17) [21,70]			0.00[2] [21,70]	0.12[2] (35000) [44]		
Sulfamerazine	0.11[2] (K17) [21,70]			0.00[2] [70]			
Sulfamethoxazole				0.13[1] [69]			
Sulfathiazole	0.27[2] (K17) [21,70]			0.07[2] [21,70]	0.22[2] (35000) [44]		
Tadalafil			0.25[3] (6:4) [13]				
Telmisartan	0.00[2] (K25) [71]		0.00[3] (6:4)	0.00[2] [71]		0.00[2] (E100) [71]	0.00[2] (E5) [71]
Temazepam	0.00[1] (K30) [72]				0.03[1] (6000) [72]		
Verapamil-HCl			0.00[3] (6:4)				

First, the sample was annealed for 1 h at a certain temperature, at which the melt viscosity of the specimen allowed the API to dissolve. Secondly, the T_g of this annealed sample was determined and a further T_g analysis of the respective amorphous system with the completely dissolved API fraction was conducted. This procedure was repeated at different API/polymer weight fractions. Further, the second analysed T_gs served for the determination of the weight fraction-dependent curve progression of T_g by employing the Brostow Chiu Kalogeras Vassilikou-Dova fit (BCKV-fit, Eq. (1)),

$$T_g = w_1 T_{g,1} + (1 - w_1) T_{g,2} + w_1(1 - w_1)[a_0 + a_1(2w_1 - 1) + a_2(2w_1 - 1)^2] \quad (1)$$

where at $T_{g,1}$ and $T_{g,2}$ are the T_gs of API and polymer, respectively, w_1 is the weight fraction of the API and a_0, a_1 and a_2 are variables [30]. Due to its polynomial form, the BCKV-fit is able to consider positive and negative deviations from the Couchman-Karasz fit [31]. Thus, it was appropriate to identify the solubilized API fraction of the annealed samples by employing the API weight fraction-dependent curve progression of glass transition temperature. Finally, for predicting the API solubility phase diagram, Eq. (2) was fitted to the solubility curve progression,

$$T_{Annealing} = y_0 + A * e^{R_0 * x} \quad (2)$$

where x is the soluble API fraction (wAPI/wpolymer) at the respective temperature, A and R0 are fitting constants and y0 corresponds to the API melting point but was set as a variable. All API solubility results were further confirmed with XRPD measurements (data not shown). In XRPD trials, API weight fraction/temperature combinations, which were on the estimated API solubility curve, were chosen to verify the presence of an entirely amorphous sample as described in detail in our previous publication [23]. XRPD proved to be more sensitive to detect remaining crystallinity compared to our DSC method. However, the soluble API weight fraction detected by DSC could be corroborated via XRPD for most cases. In the cases where XRPD detected remaining crystallinity in contrast to the DSC, a 5% lower API loading reached the amorphous state at the respective temperature in all cases.

2.2.3. Empirical model of solubility in COP

In short, to predict if the solubility in COP at 100 °C is at least 0.20 ($w_{API}/w_{polymer}$), we used R, a freely available language and environment for statistical computing and graphics [32]. Molecular descriptors of the API in COP in Table 1 of the manuscript were computed with MOE [33]. These descriptors were supplemented with data obtained from our experiments (Table 1) and from the PubChem database [29]. Features that had no value or had the same value for 50% or more of the compounds were removed. Features were not standardized at the beginning of the computations. Instead, standardization was performed prior to any model training.

An initial estimate of the necessary number of descriptors was obtained using the method Least Absolute Shrinkage and Selection Operator (LASSO) from package glmnet [34], whereas selection of features was performed using the LiblineaR package [35], which provides a wrapper for the LIBLINEAR C/C++ library for machine learning [36]. The predictive accuracy was assessed using balanced accuracy computed by the package caret [37].

Features were selected using recursive feature elimination [38]. The optimal value of the hyperparameter of each regularized logistic regression model was estimated by a leave-one out crossvalidation. To assess the predictive accuracy of our models for unseen data, we performed nested crossvalidation: in an additional outer loop we employed leave-one out crossvalidation to compute the balanced accuracy for test samples. The selection of the features for the final model was based on the full set of compounds.

A more detailed description of our approach is given in the supplementary material (Appendix A).

3. Results & discussion

The data of API solubility in polymeric matrices from literature, together with our own results, are given in Table 2. In general, solubility data were given in weight fractions ($w_{API}/w_{polymer}$). Regarding the data set, the focus was on polymers which were commonly known for their application in hot-melt extrusion and on solubility determinations, which were based on experimental results. The following polymers occurred frequently enough in literature to warrant inclusion in our compilation: polyvinylpyrrolidone grades (PVP), polyvinyl acetate (PVAc), vinylpyrrolidone-vinyl acetate copolymer (copovidone, COP), polyvinyl caprolactam-polyvinyl acetate-polyethylene glycol graft polymer (Soluplus®, SOL), different types methacrylate copolymers (PMMA), polyethylene glycol (PEG) and hydroxypropyl-methylcellulose grades (HPMC). To expand the data set, solubility data of further 20 APIs, measured either in the polymer COP or SOL, were added. In total, the final data set was comprised of 37 APIs and 2 sugar derivatives with a varying extent of available polymer data and several measuring techniques to obtain the API solubility in polymeric matrices. A detailed compilation of the physicochemical characteristics of the APIs and sugar derivatives under investigation is listed in the supplementary section (Appendix B). Although different measuring techniques were used, the majority of techniques were based on DSC. Observed differences in the solubilities for the same substance likely depended on both the measuring technique, obviously, but also on the working group which conducted the measurements.

3.1. Measuring techniques

In the data set presented in Table 2, only API solubilities which were derived from experimental values were considered. The index next to the solubility value depicts the measuring technique used. They were divided into melting point depression methods by using the onset of the melting point (T_m) (index 1), dissolution endpoint methods using the endset of T_m (index 2), indirect measurements via the glass transition temperatures (index 3), measurements in low molecular weight analogues (index 4) and further measuring techniques (index 5). The fifth category of measuring techniques includes for example, a technique based on a thermodynamic model to calculate the Gibbs energy change while forming a drug-polymer solution [24], using solution calorimetry to determine enthalpies of mixing [25] or investigating the stability of ASDs against high-energy mechanical milling [26].

3.1.1. Melting point depression method

In the case of the melting point depression method, an adequately low heating rate (approx. 0.2–2 K/min) is applied to a physical mixture and the onset of the melting endotherm characterizes the temperature which enables the dissolution of the entire API fraction [10,17,18]. Employing the Flory-Huggins lattice theory and the proposed calculation of the interaction parameter χ by Marsac et al. was able to extrapolate the API solubility to ambient temperatures using the melting point depression of a soluble API/polymer system [39,40]. One of the drawbacks of this method is that at a low crystalline API weight fraction, the melting peak becomes more broad and flat, making it challenging to define the onset accurately [10,41,42]. Furthermore, the onset only characterizes the starting point of the API dissolution within the polymeric matrix. It remains unknown whether the entire API fraction would dissolve at this temperature or probably at temperatures above the onset [43-45]. However, this method is more robust against the sample preparation method used. While for the dissolution endpoint method a certain maximal particle size of the specimen needs to be defined for an appropriate solubility determination, this drawback is less critical for the melting point depression method [19,22].

3.1.2. Dissolution endpoint method

Regarding the dissolution endpoint method, a cryo-milled physical mixture and the application of an adequately low heating rate (approx. 0.2–2 K/min) enables the accurate characterisation of the melting endotherm endset, which serves as the temperature point where the API fraction is entirely soluble within the polymeric matrix [19-21]. This method is prone to errors due to measurements in a non-equilibrated state as a result of high heating rates (> 2 K/min) or insufficiently large particle sizes, as cryo-milling seemed to be necessary for an accurate determination of the melting point endset [19,22]. Due to the strong dependency of the resulting solubility on the preparation method, this method is prone to error. The extrapolation to ambient temperature can either be performed by using the Flory-Huggins lattice theory [39,40], the empirical assumption of Kyerematen et.al. [21] or the relatively new PC-SAFT (perturbed-chain statistical associating fluid theory) software from Sadowski and co-workers, which is based on a perturbation theory for chain molecules [44,46-48]. In the case of PC-SAFT, not only binary mixtures of different API/polymer combinations were investigated [44,46], but also the influence of humidity on the long-term physical stability of ASD [47] as well as amorphous-amorphous phase separations [48] were evaluated.

3.1.3. Indirect solubility determination by T_g

Indirect measurements of the API solubility in a polymeric matrix are based on analysis of annealed or recrystallized samples [22,23]. We

employed this approach in our own studies. For detailed information, the reader is kindly referred to Section 2.2.2. In the case of the recrystallization method, a supersaturated amorphous solid dispersion is prepared by solvent evaporation and annealed at different temperatures. Subsequently, the T_g of the annealed sample is analyzed and compared to the API weight fraction-dependent course of T_g by employing the Gordon-Taylor equation [49]. Extrapolation to room temperature was conducted by employing the Flory-Huggins lattice theory [39,40]. Due to the use of the Gordon-Taylor equation to identify the soluble API weight fraction, the weight fraction-dependent course of T_g has to follow this equation. Otherwise a regression can only be performed between two measuring points which is statistically questionable [50]. However, the comparability of this indirect measurement to melting point depression techniques has already been proven [51].

3.1.4. Measurement in low molecular weight analogues

In this method, the measurement is performed in the low molecular weight analogue monomer (e.g. 1-ethyl-2-pyrrolidone instead of PVP) of a desired polymer [27,39]. Regarding copolymers, the measurements are conducted separately in the respective analogous monomers and in dependence of the composition of the copolymer, the solubility is calculated. By using a liquid analogue, the API solubility in the low molecular weight analogue can be directly determined at room temperature and it is further extrapolated to the polymer of interest. Therefore, difficulties in achieving an equilibrated state during solubility measurements of a highly viscous ASD are circumvented. However, whether the effect of the polymer's molecular weight and probable steric hindrances are negligible at all times is questionable. Hints of an existing threshold for the influence of molecular mobility have already been found [50].

3.2. Comparison of the common measuring techniques

Upon investigation of the deviation due to different measuring techniques used to obtain API solubility data, no trend was observed to rank the measuring techniques according to their reliability (Table 2). Conducting the chosen measuring technique in an accurate way to ensure the sample is in its equilibrated state during analysis seems more important than the method itself. For example, the determined solubility ($w_{API}/w_{polymer}$) of felodipine in PVP seemed more dependent on the working group who conducted the experiments than on the measuring technique itself. The felodipine-PVP (K12-K90) solubility fraction determined by using the dissolution endpoint method ranged between 0.00 and 0.24 [43,52], whereas the use of low molecular weight analogues resulted in a solubility from 0.05 to 0.31 [39,53], independent of the PVP grade used. More striking is the discrepancy in solubility data for measurements with an indomethacin-COP system by Kyerematen et al. (0.32 at 25 °C) [21] and by Knopp et al. (0.06 at 25 °C) [53], both using the dissolution endpoint method. Although they used the same methodology, the obtained indomethacin solubility varied. In comparison to other publications, the obtained solubility by Kyerematen et al. seemed more consistent (Table 2) than the one of Knopp et al., leaving the accuracy in solubility determination in the last case questionable.

3.3. Consistency within the obtained literature data set

To evaluate the consistency within the solubility data in Table 2, APIs with a wide set of available data were chosen, namely acetaminophen, celecoxib, felodipine, indomethacin, naproxen and nifedipine. In most of the cases, the largest data sets were obtained for PVP and COP, therefore these two polymers served as the basis to judge the accuracy of solubility results.

In the case of acetaminophen, the solubility data were mainly derived by Rades and co-workers [53,54] or by Sadowski and co-workers [21,47,55]. Regarding the solubility of acetaminophen-PVP, it varied from 0.17 to 0.32, whereas the API was insoluble in PVAc. Consequently, the solubility in COP (6:4) decreased slightly to 0.21–0.28, compared to PVP. A further COP grade (3:7) with a lower PVP content led to a further reduction in solubility to 0.02–0.05. Therefore, a consistent data set in terms of acetaminophen could be presented, but with a slight variation in acetaminophen-PVP solubility. Regarding celecoxib, the entire data set for PVP, PVAc and COP was found in publications from Rades and co-workers [50,51,53,54], except two data points of our own work in COP and SOL. Our measured COP solubility was in good agreement with literature. However, the solubility in SOL seemed to be underestimated by our own approach. In general, celecoxib was found to be soluble in most of the investigated polymers, but its solubility in PVAc might be very low. In the case of felodipine, a wide data set reported by a variety of authors was found, namely the obtained solubility in PVP ranged from 0.00 to 0.31. Due to the low solubility in PVAc and the average solubility of 0.21 in COP, the higher solubilities in PVP might be more consistent with the overall data set. Furthermore, our results for the felodipine-COP system were in good accordance with the overall data set. For indomethacin, a comparably large data set to felodipine was obtained. As mentioned above for other APIs, the solubility in PVP was highly variable (0.08–0.54), which makes it difficult to comment about the solubility of indomethacin in PVP. However, the solubility in COP (6:4, PVP:PVAc) was reported in a narrow range of 0.31–0.36. Due to the insoluble indomethacin-PVAc system, a PVP-solubility which was higher than the COP-solubility would be plausible. In the case of naproxen, mainly two groups of authors had worked on its solubility, Paudel et al. [17] and Sadowski and co-workers [21,47,55]. Paudel et al. determined a solubility in PVP of 0.06 for naproxen, whereas the group of Sadowski exceeded a solubility of 0.31 to 0.36. With respect to the low solubility in PVAc and in comparison to the results for COP (6:4) in the range of 0.19–0.28, in which our own data point was included, the higher solubility of Sadowski and co-workers seemed more reliable. Regarding nifedipine, data from Marsac et al. (0.05–0.07 in PVP) [27,28], Kyerematen et al. (0.21 in PVP, 0.12 in COP) [21] and solubility of our own investigations (0.19 in COP) were obtained. Similar to the afore-mentioned APIs in PVP or COP, for a nifedipine-PVP system a solubility around 0.21 seems more plausible than a lower value. Otherwise due to the insoluble nifedipine-PVAc system, the present solubility in COP would be unexplainably high. Furthermore, our determined solubility in COP (0.19) was in good accordance to literature values [21].

To conclude, in most of the regarded cases, a higher solubility in the respective polymer seemed to be more plausible than lower findings. The underestimation of API solubility might be a reason of measurements in a non-equilibrated state of the system under investigation. Therefore, before conducting measurements, the kinetic factor of melt viscosity must be considered, and it has to be assured that this is not influencing the desired solubility determination.

3.4. Solubility in polymer-dependency

The focus for this data review was on polymers which can be used to form ASD, either by spray-drying or by HME, namely PVP, PVAc, COP, SOL, PMMA, PEG and HPMC (Table 2). The largest data set was obtained for the various PVP grades, followed by COP, SOL and PVAc. Only limited publications were found for PMMA, PEG and HPMC.

For PVP, a variety of molecular weight grades from K12 (approx. 2,500 g/mol) to K90 (approx. 1,250,000 g/mol) were investigated. In general, no connection or tendency between molecular weight and API solubility could be made, which might be also a fact of the high spectrum in API solubility found in literature. However, PVP was the polymer which enabled the highest API solubility throughout the investigated polymers due to its high ability to form hydrogen bonds [56]. The highest solubility in PVP was found for celecoxib (up to 0.60), indomethacin (up to 0.54) and chloramphenicol (up to 0.52) [50,51,53]. In contrast, most APIs were sparely soluble in PVAc, due to

the lack of specific interactions, especially hydrogen bonding [56]. The API solubility in PVAc did not exceeded 0.1 for the entire data set, except for celecoxib where a solubility of up to 0.16 was reported [54]. Regarding copovidone COP, consisting of PVP and PVAc in different weight ratios, the API solubility was slightly decreased in comparison to PVP. Furthermore, a decrease in PVP weight ratios always went hand in hand with a further reduction in the respective API solubility [46,50,57]. Therefore, regarding APIs in COP, the solubility of an API mainly depended on the hydrogen bonding capability of PVP, whereas PVAc seemed more important for the processability of the copolymer than for improving the API solubility.

In the case of SOL, similar API solubilities compared to COP were achieved. The highest solubilities in SOL were found for celecoxib (0.34) naproxen (0.32) and indomethacin (0.31) [51]. Regarding the structure of SOL, it consists inter alia of PEG and PVAc units. As already stated, PVAc was sparely able to form specific interactions, e.g. hydrogen bonding, with a desired API. Thus, instead of the PVAc part, the PEG in SOL might be influencing or promoting the API solubility. In the case of indomethacin, the API solubilities in PEG (0.22–0.25) and SOL (0.20–0.31) were comparable. Furthermore, ketoconazole was insoluble in both polymers. However, discrepancies in solubility for sulfadimidine (SOL 0.00; PEG 0.12) and sulfathiazole (SOL 0.07; PEG 0.22) were found. Thus, due to the limits in the data set, no statement about the solubility-dependent polymer parts in SOL could be made, except that the PVAc fraction is unlikely to improve the API solubility. For PMMA and HPMC, again only a limited data set was found, which hindered any evaluation. However, the solubility in PMMA or HPMC was always lower or comparable to PVP.

3.5. Empirical model of solubility in COP

We developed an empirical model to predict if the solubility of a given compound in COP is at least 20% at 100 °C. For this purpose, we (i) generated a table containing experimental and computed properties of the compounds, (ii) performed an initial assessment of the number of features necessary to separate the two classes of compounds, (iii) estimated the predictive ability of models trained using recursive feature elimination by cross-validation and (iv) applied recursive feature elimination on the full dataset.

Our table used for feature selection contained a total of 146 features. The number of features necessary to separate compounds exhibiting 0.2 ($w_{API}/w_{polymer}$) solubility at 100 °C in COP from those that are less soluble was estimated to be 12. In detail, the following features were selected from all available features (sorted by rank): PEOE_VSA_FPNEG, BCUT_SLOGP_0, std_dim2, b_rotR, a_don, SlogP_VSA6, E_tor, balabanJ, T_g, dens, SlogP_VSA8, E_ang. Of these only T_g is an experimentally determined value. All other features are descriptors computed by the MOE program. In the next step, we estimated the dependency of the predictive ability of our final model on the number of features by plotting the balanced accuracy of the models obtained by leave-one-out cross-validation (Fig. 1). The features used by the models were determined by recursive feature elimination, that is, all features used by a given model are contained in models with higher cardinality. This plot indicates that the balanced accuracy levels off at 71% with 8 features, which is clearly better than a random model that would achieve a balanced accuracy of only 50%. Further evaluation of the results using up to 12 features showed that celecoxib, dipyridamole, gliclazide, lamotrigine, loratadine and probucol were mispredicted in many cases. This hints at the existence of at least two clusters of compounds, since celecoxib, dipyridamole, gliclazide and lamotrigine were the only APIs with a positive deviation from the Couchman-Karasz equation [31] in the investigated data set. However, the connection between misprediction and positive deviation from Couchman-Karasz fit remained unclear and could not be ascribed to a solubility measuring issue.

Finally, performing recursive feature elimination using all compounds led to the feature selection depicted in Table 3 (sorted by rank). Using this set of features results in a training error of zero for the full dataset. In this model, the glass transition temperature has a negative effect on solubility in COP at 100 °C, whereas the number hydrogen bond donor atoms seems to enhance the solubility. The coefficients of this model are given in Table A.1 in the supplementary part.

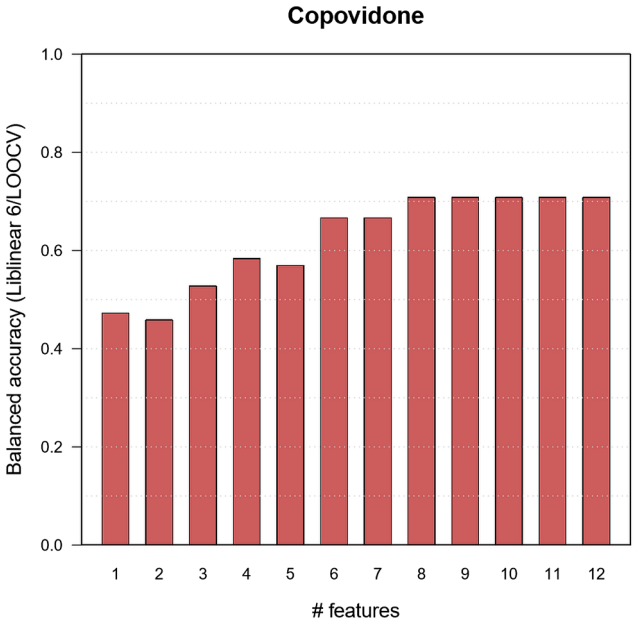

Fig. 1. Balanced accuracy for unseen data obtained by recursive feature elimination versus the number of features used by the models.

Since two different approaches were used in selecting the set given above and the one given in Table 3, differences between the two sets are possible. The LASSO method aims at balancing the accuracy and simplicity of the model. Recursive feature elimination, on the other hand, starts with a model containing all features and tries to improve generalization performance by recursively removing the feature having the least effect on the training error of the current model. Furthermore, based on the balanced accuracy plot, we constrained the number of features to be selected by recursive feature elimination to 8, whereas the LASSO method selected 12 features.

However, there is an overlap between both sets of selected features: 7 of the 8 features selected by recursive feature elimination were also selected by the LASSO method. More specifically, the features selected by both methods were a_don, SlogP_VSA8, T_g, PEOE_VSA_FPNEG, b_rotR, SlogP_VSA6 and BCUT_SLOGP_0. Some of the computed features are of special interest. For example, both the number of hydrogen bond donor atoms (a_don) and the fractional negative polar van der Waals surface area (PEOE_VSA_FPNEG) may be important to describe the interaction between the compound and COP. b_rotR is the number of rotatable bonds divided by the total number of bonds and hence encodes information about the flexibility of the molecule. Interestingly,

Table 3
Description of the selected features (sorted by rank) for solubility prediction.

Rank	Feature	Description
(1)	a_don	Number of H-bond donor atoms
(2)	SlogP_VSA8	Related to the hydrophobicity of the molecule
(3)	T_g	Experimentally determined glass transition temperature
(4)	PEOE_VSA_FPNEG	Fractional negative polar van der Waals surface area
(5)	E_oop	Out-of-plane potential energy
(6)	b_rotR	Fraction of rotatable bonds
(7)	SlogP_VSA6	Related to the hydrophobicity of the molecule
(8)	BCUT_SLOGP_0	Related to the hydrophobicity of the molecule

the experimentally determined glass transition temperature (T_g) is selected in both approaches as well. Using only these 4 features, instead of using the total number of 8 features determined by recursive feature elimination as reported above, results in misclassification of three compounds in the training set (Celecoxib, Cilostazol and Gliclazide). The coefficients of this reduced model are given in Table A.1 in the supplementary part.

Further computations need to be carried out to confirm the existence of different subgroups of compounds (e.g. positive deviation from Couchman-Karasz fit as indicator) and whether the set of four features may be replaced by other combinations with the same or even a lower cardinality.

4. Conclusion

We compiled data available in literature on API solubility in polymers. The final data set comprises seven polymers (PVP, PVAc, COP, SOL, PEG, PMMA and HPMC), 37 APIs and two sugar derivatives in total. It also includes our own so far unpublished data set which was found to be consistent with previously published data. The majority of studies used the melting point depression method, dissolution endpoint measurements, indirect solubility determination by T_g or low molecular weight analogues. It appears that the resulting API solubility depended not only on the method used, but rather more on the working group and authors who conducted the measurements. The API solubility measurement itself is prone to bias due to difficulties in reaching the equilibrated state of a system prior any solubility determination. Hence, working group-specific analytical methods, once inadequately chosen, seemed to be maintained. In general, all techniques exhibited advantages and disadvantages, leading to no superior measurement technique. The selection of a measuring technique should be based on the purpose of ASD formation, on the later selected manufacturing process to form such an ASD (e.g. HME or spray-drying), and the available equipment to conduct API solubility determination. The accuracy of the method performed should be further assessed by comparison with published data for which this publication serves as a guidance.

Furthermore, no simple relation between API solubility and the molecular weight of PVP was observed. PVP always exhibited the highest API solubility, whereas APIs showed the poorest solubility in PVAc. This is underlined by the findings for COP, a copolymer of PVP and PVAc. Here, the API solubility changes as a function of the PVP/PVAc ratio. Only a limited number of publications were found for PEG, PMMA and HPMC and therefore no statement considering these polymers can be made. In conclusion, a comparison of the available data set and models in literature on the API solubility prediction in polymeric matrices has been made. Using the example of COP we have shown that the data now available may be utilized in developing fast computational models to assess the solubility in polymers. In summary, this data review should assist researchers in choosing an estimation method suited for their studies and the data set presented here should facilitate training newly developed solubility prediction models.

Furthermore, a statistical assessment to identify descriptors of molecules, which are connected to the API solubility in polymeric matrices, was successfully performed. In particular, 8 descriptors in total, namely number of hydrogen bonding donors, three descriptors related to the hydrophobicity of the molecule, glass transition temperature, fractional negative polar van der Waals surface area, out-of-plane potential energy and the fraction of rotatable bonds correlated with the API solubility. Furthermore, API which showed a positive deviation from the theoretical Couchman-Karasz API fraction-dependent T_g-curve, were incorrectly predicted in many cases, leading to the conclusion of at least to clusters of compounds. The statistical model used is able to predict the criterium 20% API soluble at 100 °C (Yes/No) for an unknown compound with a balanced accuracy of 71%. This statistical assessment underlines the importance and utility of a large and valuable data set to perform statistical evaluations upon API solubility in polymeric matrices.

Acknowledgement

The authors would like to thank Rachel C. Evans greatly for reviewing the manuscript. During the conduction of this research, Andreas Gryczke was employed by BASF SE (Ludwigshafen am Rhein, 67063, Germany) and Esther S. Bochmann was employed by the University of Bonn. This research did not receive any specific grant from funding agencies in the public, commercial, or not-for-profit sectors.

Appendix A. Supplementary material

Supplementary data to this article can be found online at https://doi.org/10.1016/j.ejpb.2019.05.012.

References

[1] H. Liu, L.S. Taylor, K.J. Edgar, The role of polymers in oral bioavailability enhancement; a review, Polymer (2015), https://doi.org/10.1016/j.polymer.2015.09.026.
[2] Y. He, C. Ho, Amorphous solid dispersions: utilization and challenges in drug discovery and development, J. Pharm. Sci. 104 (2015) 3237–3258, https://doi.org/10.1002/jps.24541.
[3] S. Janssens, G. Van den Mooter, Review: physical chemistry of solid dispersions, J. Pharm. Pharmacol. 61 (2009) 1571–1586, https://doi.org/10.1211/jpp/61.12.0001.
[4] N. Ogawa, T. Hiramatsu, R. Suzuki, R. Okamoto, K. Shibagaki, K. Fujita, C. Takahashi, Y. Kawashima, H. Yamamoto, Improvement in the water solubility of drugs with a solid dispersion system by spray drying and hot-melt extrusion with using the amphiphilic polyvinyl caprolactam-polyvinyl acetate-polyethylene glycol graft copolymer and d -mannitol, Eur. J. Pharm. Sci. 111 (2018) 205–214, https://doi.org/10.1016/j.ejps.2017.09.014.
[5] J.A. Baird, L.S. Taylor, Evaluation of amorphous solid dispersion properties using thermal analysis techniques, Adv. Drug Deliv. Rev. 64 (2012) 396–421, https://doi.org/10.1016/j.addr.2011.07.009.
[6] B.C. Hancock, M. Parks, What is the true solubility advantage for amorphous pharmaceuticals? Pharm. Res. 17 (2000) 397–404.
[7] S.B. Murdande, M.J. Pikal, R.M. Shanker, R.H. Bogner, Solubility advantage of amorphous pharmaceuticals: II. application of quantitative thermodynamic relationships for prediction of solubility enhancement in structurally diverse insoluble pharmaceuticals, Pharm. Res. 27 (2010) 2704–2714, https://doi.org/10.1007/s11095-010-0269-5.
[8] S. Huang, C. Mao, R.O. Williams, C.-Y. Yang, Solubility advantage (and disadvantage) of pharmaceutical amorphous solid dispersions, J. Pharm. Sci. 105 (2016) 3549–3561, https://doi.org/10.1016/j.xphs.2016.08.017.
[9] S. Baghel, H. Cathcart, N.J. O'Reilly, Polymeric amorphous solid dispersions: a review of amorphization, crystallization, stabilization, solid-state characterization, and aqueous solubilization of biopharmaceutical classification system class II drugs, J. Pharm. Sci. 105 (2016) 2527–2544, https://doi.org/10.1016/j.xphs.2015.10.008.
[10] J. Gupta, C. Nunes, S. Vyas, S. Jonnalagadda, Prediction of solubility parameters and miscibility of pharmaceutical compounds by molecular dynamics simulations, J. Phys. Chem. B. 115 (2011) 2014–2023, https://doi.org/10.1021/jp108540n.
[11] M. Vasanthavada, W.-Q. (Tony) Tong, Y. Joshi, M.S. Kislalioglu, Phase behavior of amorphous molecular dispersions II: role of hydrogen bonding in solid solubility and phase separation kinetics, Pharm. Res. 22 (2005) 440–448, https://doi.org/10.1007/s11095-004-1882-y.
[12] F. Qian, J. Huang, M.A. Hussain, Drug-polymer solubility and miscibility: stability consideration and practical challenges in amorphous solid dispersion development, J. Pharm. Sci. (2010) n/a-n/a, https://doi.org/10.1002/jps.22074.
[13] K. Wlodarski, W. Sawicki, A. Kozyra, L. Tajber, Physical stability of solid dispersions with respect to thermodynamic solubility of tadalafil in PVP-VA, Eur. J. Pharm. Biopharm. 96 (2015) 237–246, https://doi.org/10.1016/j.ejpb.2015.07.026.
[14] P. Piccinni, Y. Tian, A. McNaughton, J. Fraser, S. Brown, D.S. Jones, S. Li, G.P. Andrews, Solubility parameter-based screening methods for early-stage formulation development of itraconazole amorphous solid dispersions, J. Pharm. Pharmacol. 68 (2016) 705–720, https://doi.org/10.1111/jphp.12491.
[15] F. Meng, V. Dave, H. Chauhan, Qualitative and quantitative methods to determine miscibility in amorphous drug–polymer systems, Eur. J. Pharm. Sci. 77 (2015) 106–111, https://doi.org/10.1016/j.ejps.2015.05.018.
[16] B. Tian, X. Wang, Y. Zhang, K. Zhang, Y. Zhang, X. Tang, Theoretical prediction of a phase diagram for solid dispersions, Pharm. Res. (2014), https://doi.org/10.1007/s11095-014-1500-6.
[17] A. Paudel, J. Van Humbeeck, G. Van den Mooter, Theoretical and experimental investigation on the solid solubility and miscibility of naproxen in poly(vinylpyrrolidone), Mol. Pharm. 7 (2010) 1133–1148, https://doi.org/10.1021/mp100013p.

[18] Y. Zhao, P. Inbar, H.P. Chokshi, A.W. Malick, D.S. Choi, Prediction of the thermal phase diagram of amorphous solid dispersions by flory-huggins theory, J. Pharm. Sci. 100 (2011) 3196–3207, https://doi.org/10.1002/jps.22541.
[19] J. Tao, Y. Sun, G.G.Z. Zhang, L. Yu, Solubility of small-molecule crystals in polymers: d-mannitol in PVP, indomethacin in PVP/VA, and nifedipine in PVP/VA, Pharm. Res. 26 (2009) 855–864, https://doi.org/10.1007/s11095-008-9784-z.
[20] Y. Sun, J. Tao, G.G.Z. Zhang, L. Yu, Solubilities of crystalline drugs in polymers: an improved analytical method and comparison of solubilities of indomethacin and nifedipine in PVP, PVP/VA, and PVAc, J. Pharm. Sci. (2010) n/a-n/a, https://doi.org/10.1002/jps.22251.
[21] S.O. Kyerematen, M. Pudlas, G.H. Woehrle, A fast and reliable empirical approach for estimating solubility of crystalline drugs in polymers for hot melt extrusion formulations, J. Pharm. Sci. 103 (2014) 2847–2858, https://doi.org/10.1002/jps.23941.
[22] A. Mahieu, J.-F. Willart, E. Dudognon, F. Danède, M. Descamps, A new protocol to determine the solubility of drugs into polymer matrixes, Mol. Pharm. 10 (2013) 560–566, https://doi.org/10.1021/mp3002254.
[23] E.S. Bochmann, D. Neumann, A. Gryczke, K.G. Wagner, Micro-scale prediction method for API-solubility in polymeric matrices and process model for forming amorphous solid dispersion by hot-melt extrusion, Eur. J. Pharm. Biopharm. 107 (2016) 40–48, https://doi.org/10.1016/j.ejpb.2016.06.015.
[24] R.A. Bellantone, P. Patel, H. Sandhu, D.S. Choi, D. Singhal, H. Chokshi, A.W. Malick, N. Shah, A method to predict the equilibrium solubility of drugs in solid polymers near room temperature using thermal analysis, J. Pharm. Sci. 101 (2012) 4549–4558, https://doi.org/10.1002/jps.23319.
[25] J. Alin, N. Setiawan, M. Defrese, J. DiNunzio, H. Lau, L. Lupton, H. Xi, Y. Su, H. Nie, N. Hesse, L.S. Taylor, P.J. Marsac, A novel approach for measuring room temperature enthalpy of mixing and associated solubility estimation of a drug in a polymer matrix, Polymer 135 (2018) 50–60, https://doi.org/10.1016/j.polymer.2017.11.056.
[26] Z. Yang, K. Nollenberger, J. Albers, S. Qi, Molecular implications of drug-polymer solubility in understanding the destabilization of solid dispersions by milling, Mol. Pharm. 11 (2014) 2453–2465, https://doi.org/10.1021/mp500205c.
[27] P.J. Marsac, T. Li, L.S. Taylor, Estimation of drug-polymer miscibility and solubility in amorphous solid dispersions using experimentally determined interaction parameters, Pharm. Res. 26 (2009) 139–151, https://doi.org/10.1007/s11095-008-9721-1.
[28] P.J. Marsac, H. Konno, L.S. Taylor, A Comparison of the Physical Stability of Amorphous Felodipine and Nifedipine Systems, Pharm. Res. 23 (2006) 2306–2316, https://doi.org/10.1007/s11095-006-9047-9.
[29] S. Kim, P.A. Thiessen, E.E. Bolton, J. Chen, G. Fu, A. Gindulyte, L. Han, J. He, S. He, B.A. Shoemaker, J. Wang, B. Yu, J. Zhang, S.H. Bryant, PubChem Substance and Compound databases, Nucleic Acids Res. 44 (2016) D1202–D1213, https://doi.org/10.1093/nar/gkv951.
[30] W. Brostow, R. Chiu, I.M. Kalogeras, A. Vassilikou-Dova, Prediction of glass transition temperatures: binary blends and copolymers, Mater. Lett. 62 (2008) 3152–3155, https://doi.org/10.1016/j.matlet.2008.02.008.
[31] P.R. Couchman, F.E. Karasz, A classical thermodynamic discussion of the effect of composition on glass-transition temperatures, Macromolecules. 11 (1978) 117–119.
[32] R Core Team, R: A Language and Environment for Statistical Computing, R Foundation for Statistical Computing, Vienna, Austria, 2018. < https://www.R-project.org/ > .
[33] Molecular Operating Environment (MOE), Chemical Computing Group ULC, 1010 Sherbooke St. West, Suite #910, Montreal, QC, Canada, H3A 2R7, 2018.
[34] J. Friedman, T. Hastie, R. Tibshirani, Regularization paths for generalized linear models via coordinate descent, J. Stat. Softw. 33 (2010) 1–22.
[35] T. Helleputte, LiblineaR: Linear Predictive Models Based on the LIBLINEAR C/C++ Library, 2017.
[36] R.-E. Fan, K.-W. Chang, C.-J. Hsieh, X.-R. Wang, C.-J. Lin, LIBLINEAR: a library for large linear classification, J Mach Learn Res. 9 (2008) 1871–1874.
[37] M.K.C. from J. Wing, S. Weston, A. Williams, C. Keefer, A. Engelhardt, T. Cooper, Z. Mayer, B. Kenkel, the R.C. Team, M. Benesty, R. Lescarbeau, A. Ziem, L. Scrucca, Y. Tang, C. Candan, T. Hunt, caret: Classification and Regression Training, 2018. < https://CRAN.R-project.org/package=caret > .
[38] I. Guyon, J. Weston, S. Barnhill, V. Vapnik, Gene selection for cancer classification using support vector machines, Mach. Learn. 46 (2002) 389–422, https://doi.org/10.1023/A:1012487302797.
[39] P.J. Marsac, S.L. Shamblin, L.S. Taylor, Theoretical and practical approaches for prediction of drug-polymer miscibility and solubility, Pharm. Res. 23 (2006) 2417–2426, https://doi.org/10.1007/s11095-006-9063-9.
[40] P.J. Flory, Principles of polymer chemistry, 19. print, Cornell Univ. Press, Ithaca, NY, 2006.
[41] S. Thakral, N.K. Thakral, Prediction of drug-polymer miscibility through the use of solubility parameter based flory-huggins interaction parameter and the experimental validation: PEG as model polymer, J. Pharm. Sci. 102 (2013) 2254–2263, https://doi.org/10.1002/jps.23583.
[42] J. Djuris, I. Nikolakakis, S. Ibric, Z. Djuric, K. Kachrimanis, Preparation of carbamazepine–Soluplus® solid dispersions by hot-melt extrusion, and prediction of drug–polymer miscibility by thermodynamic model fitting, Eur. J. Pharm. Biopharm. 84 (2013) 228–237, https://doi.org/10.1016/j.ejpb.2012.12.018.
[43] C. Donnelly, Y. Tian, C. Potter, D.S. Jones, G.P. Andrews, Probing the effects of experimental conditions on the character of drug-polymer phase diagrams constructed using flory-huggins theory, Pharm. Res. 32 (2015) 167–179, https://doi.org/10.1007/s11095-014-1453-9.
[44] A. Prudic, Y. Ji, G. Sadowski, Thermodynamic phase behavior of API/polymer solid dispersions, Mol. Pharm. 11 (2014) 2294–2304, https://doi.org/10.1021/mp400729x.
[45] M. Yang, P. Wang, H. Suwardie, C. Gogos, Determination of acetaminophen's solubility in poly(ethylene oxide) by rheological, thermal and microscopic methods, Int. J. Pharm. 403 (2011) 83–89, https://doi.org/10.1016/j.ijpharm.2010.10.026.
[46] A. Prudic, T. Kleetz, M. Korf, Y. Ji, G. Sadowski, Influence of copolymer composition on the phase behavior of solid dispersions, Mol. Pharm. 11 (2014) 4189–4198, https://doi.org/10.1021/mp500412d.
[47] K. Lehmkemper, S.O. Kyerematen, O. Heinzerling, M. Degenhardt, G. Sadowski, Long-term physical stability of PVP- and PVPVA-amorphous solid dispersions, Mol. Pharm. 14 (2017) 157–171, https://doi.org/10.1021/acs.molpharmaceut.6b00763.
[48] C. Luebbert, F. Huxoll, G. Sadowski, Amorphous-amorphous phase separation in API/polymer formulations, Molecules. 22 (2017) 296, https://doi.org/10.3390/molecules22020296.
[49] M. Gordon, J.S. Taylor, Ideal copolymers and the second-order transitions of synthetic rubbers. I. non-crystalline copolymers, J. Appl. Chem. 2 (1952) (1952) September.
[50] M.B. Rask, M.M. Knopp, N.E. Olesen, R. Holm, T. Rades, Influence of PVP/VA copolymer composition on drug–polymer solubility, Eur. J. Pharm. Sci. 85 (2016) 10–17, https://doi.org/10.1016/j.ejps.2016.01.026.
[51] M.B. Rask, M.M. Knopp, N.E. Olesen, R. Holm, T. Rades, Comparison of two DSC-based methods to predict drug-polymer solubility, Int. J. Pharm. 540 (2018) 98–105, https://doi.org/10.1016/j.ijpharm.2018.02.002.
[52] C. Luebbert, G. Sadowski, Moisture-induced phase separation and recrystallization in amorphous solid dispersions, Int. J. Pharm. 532 (2017) 635–646, https://doi.org/10.1016/j.ijpharm.2017.08.121.
[53] M.M. Knopp, L. Tajber, Y. Tian, N.E. Olesen, D.S. Jones, A. Kozyra, K. Löbmann, K. Paluch, C.M. Brennan, R. Holm, A.M. Healy, G.P. Andrews, T. Rades, Comparative study of different methods for the prediction of drug-polymer solubility, Mol. Pharm. 12 (2015) 3408–3419, https://doi.org/10.1021/acs.molpharmaceut.5b00423.
[54] M.M. Knopp, N. Gannon, I. Porsch, M.B. Rask, N.E. Olesen, P. Langguth, R. Holm, T. Rades, A promising new method to estimate drug-polymer solubility at room temperature, J. Pharm. Sci. 105 (2016) 2621–2624, https://doi.org/10.1016/j.xphs.2016.02.017.
[55] K. Lehmkemper, S.O. Kyerematen, O. Heinzerling, M. Degenhardt, G. Sadowski, Impact of polymer type and relative humidity on the long-term physical stability of amorphous solid dispersions, Mol. Pharm. 14 (2017) 4374–4386, https://doi.org/10.1021/acs.molpharmaceut.7b00492.
[56] K. Kothari, V. Ragoonanan, R. Suryanarayanan, The role of drug-polymer hydrogen bonding interactions on the molecular mobility and physical stability of nifedipine solid dispersions, Mol. Pharm. 12 (2015) 162–170, https://doi.org/10.1021/mp5005146.
[57] T. Matsumoto, G. Zografi, Physical properties of solid molecular dispersions of indomethacin with poly(vinylpyrrolidone) and poly(vinylpyrrolidone-co-vinylacetate) in relation to indomethacin crystallization, Pharm. Res. 16 (1999) 1722–1728.
[58] K. Bansal, U.S. Baghel, S. Thakral, Construction and validation of binary phase diagram for amorphous solid dispersion using flory-huggins theory, AAPS PharmSciTech. (2015), https://doi.org/10.1208/s12249-015-0343-8.
[59] S. Hengsawas Surasarang, J.M. Keen, S. Huang, F. Zhang, J.W. McGinity, R.O. Williams, Hot melt extrusion versus spray drying: hot melt extrusion degrades albendazole, Drug Dev Ind. Pharm. 43 (2017) 797–811, https://doi.org/10.1080/03639045.2016.1220577.
[60] S. Verma, V.S. Rudraraju, A systematic approach to design and prepare solid dispersions of poorly water-soluble drug, AAPS PharmSciTech 15 (2014) 641–657, https://doi.org/10.1208/s12249-014-0093-z.
[61] S. Baghel, H. Cathcart, N.J. O'Reilly, Theoretical and experimental investigation of drug-polymer interaction and miscibility and its impact on drug supersaturation in aqueous medium, Eur. J. Pharm. Biopharm. 107 (2016) 16–31, https://doi.org/10.1016/j.ejpb.2016.06.024.
[62] F. Meng, A. Trivino, D. Prasad, H. Chauhan, Investigation and correlation of drug polymer miscibility and molecular interactions by various approaches for the preparation of amorphous solid dispersions, Eur. J. Pharm. Sci. 71 (2015) 12–24, https://doi.org/10.1016/j.ejps.2015.02.003.
[63] Y. Tian, D.S. Jones, G.P. Andrews, An investigation into the role of polymeric carriers on crystal growth within amorphous solid dispersion systems, Mol. Pharm. 12 (2015) 1180–1192, https://doi.org/10.1021/mp500702s.
[64] S. Li, Y. Tian, D.S. Jones, G.P. Andrews, Optimising drug solubilisation in amorphous polymer dispersions: rational selection of hot-melt extrusion processing parameters, AAPS PharmSciTech 17 (2016) 200–213, https://doi.org/10.1208/s12249-015-0450-6.
[65] A. Forster, J. Hempenstall, I. Tucker, T. Rades, Selection of excipients for melt extrusion with two poorly water-soluble drugs by solubility parameter calculation and thermal analysis, Int. J. Pharm. 226 (2001) 147–161.
[66] M.M. Knopp, N.E. Olesen, P. Holm, P. Langguth, R. Holm, T. Rades, Influence of polymer molecular weight on drug-polymer solubility: a comparison between experimentally determined solubility in PVP and prediction derived from solubility in monomer, J. Pharm. Sci. 104 (2015) 2905–2912, https://doi.org/10.1002/jps.24410.
[67] X. Wang, A. Michoel, G. Van den Mooter, Study of the phase behavior of polyethylene glycol 6000–itraconazole solid dispersions using DSC, Int. J. Pharm. 272 (2004) 181–187, https://doi.org/10.1016/j.ijpharm.2003.11.026.
[68] Y. Chen, S. Wang, S. Wang, C. Liu, C. Su, M. Hageman, M. Hussain, R. Haskell, K. Stefanski, F. Qian, Initial drug dissolution from amorphous solid dispersions controlled by polymer dissolution and drug-polymer interaction, Pharm. Res. 33 (2016) 2445–2458, https://doi.org/10.1007/s11095-016-1969-2.
[69] M.A. Altamimi, S.H. Neau, Use of the flory-huggins theory to predict the solubility

of nifedipine and sulfamethoxazole in the triblock, graft copolymer soluplus, Drug Dev. Ind. Pharm. 42 (2016) 446–455, https://doi.org/10.3109/03639045.2015.1075033.

[70] V. Caron, Y. Hu, L. Tajber, A. Erxleben, O.I. Corrigan, P. McArdle, A.M. Healy, Amorphous solid dispersions of sulfonamide/soluplus® and sulfonamide/PVP prepared by ball milling, AAPS PharmSciTech. 14 (2013) 464–474, https://doi.org/10.1208/s12249-013-9931-7.

[71] R. Dukeck, P. Sieger, P. Karmwar, Investigation and correlation of physical stability, dissolution behaviour and interaction parameter of amorphous solid dispersions of telmisartan: a drug development perspective, Eur. J. Pharm. Sci. 49 (2013) 723–731, https://doi.org/10.1016/j.ejps.2013.05.003.

[72] G. Van den Mooter, P. Augustijns, N. Blaton, R. Kinget, Physico-chemical characterization of solid dispersions of temazepam with polyethylene glycol 6000 and PVP K30, Int. J. Pharm. 164 (1998) 67–80.